

Journal of
Micro/Nanolithography,
MEMS, and MOEMS

Nanolithography.SPIEDigitalLibrary.org

Correction of resist heating effect on variable shaped beam mask writer

Noriaki Nakayamada
Mizuna Suganuma
Haruyuki Nomura
Yasuo Kato
Takashi Kamikubo
Munehiro Ogasawara
Harold Zable
Yukihiro Masuda
Aki Fujimura

Noriaki Nakayamada, Mizuna Suganuma, Haruyuki Nomura, Yasuo Kato, Takashi Kamikubo, Munehiro Ogasawara, Harold Zable, Yukihiro Masuda, Aki Fujimura, "Correction of resist heating effect on variable shaped beam mask writer," *J. Micro/Nanolith. MEMS MOEMS* **15**(2), 021012 (2016), doi: 10.1117/1.JMM.15.2.021012.

SPIE.

Correction of resist heating effect on variable shaped beam mask writer

Noriaki Nakayamada,^{a,*} Mizuna Suganuma,^a Haruyuki Nomura,^a Yasuo Kato,^a Takashi Kamikubo,^a Munehiro Ogasawara,^a Harold Zable,^b Yukihiko Masuda,^b and Aki Fujimura^b

^aNuFlare Technology Inc., 8-1 Shinsugita-cho, Isogo-ku, Yokohama 235-8522, Japan

^bD2S Inc., 4040 Moorpark Avenue, San Jose, California 95117, United States

Abstract. The specifications for critical dimension (CD) accuracy and line edge roughness are getting tighter to promote every photomask manufacturer to choose electron beam resists of lower sensitivity. When the resist is exposed by too many electrons, it is excessively heated up to have higher sensitivity at a higher temperature, which results in degraded CD uniformity. This effect is called “resist heating effect” and is now the most critical error source in CD control on a variable shaped beam (VSB) mask writer. We have developed an on-tool, real-time correction system for the resist heating effect. The system is composed of correction software based on a simple thermal diffusion model and computational hardware equipped with more than 100 graphical processing unit chips. We have demonstrated that the designed correction accuracy was obtained and the runtime of correction was sufficiently shorter than the writing time. The system is ready to be deployed for our VSB mask writers to retain the writing time as short as possible for lower sensitivity resists by removing the need for increased pass count. © 2016 Society of Photo-Optical Instrumentation Engineers (SPIE) [DOI: 10.1117/1.JMM.15.2.021012]

Keywords: electron; beam; lithography; photomask; resist; heating.

Paper 15171SSP received Nov. 5, 2015; accepted for publication Mar. 7, 2016; published online Mar. 23, 2016.

1 Introduction

The shot count of a variable shaped beam (VSB) in mask writing is ever increasing along with the progress in design node and with the advancements in inverse lithography technology and extreme ultraviolet lithography. On the other hand, the entire chip (die) area on a photomask does not change drastically as it cannot be bigger than the size of the photomask. This means that the average shot size is getting smaller which increases the “shot noise.” Shot noise is the statistical variability of the number of electrons given by one VSB shot, and it is an essential source of critical dimension (CD) error and degraded line edge roughness (LER). To reduce the shot noise to get a better CD accuracy and smaller LER, one has to increase the number of electrons, i.e., the exposure dose to counteract the shrinkage in the shot size.

As the VSB shot count and exposure dose grow simultaneously, the write time also grows more rapidly and unlimitedly. The most fundamental strategy to cope with the ever aggravating write time issue by the single-beam VSB writer has been to consistently increase the electron current density. However, the combined usage of increased exposure dose and increased electron current density introduces another problem in CD control, namely the “resist heating effect.”

The resist heating problem has been known from the beginning of the development of electron beam lithography. Figure 1 is a conceptual view of the severity of the resist heating effect versus temperature. When the temperature gets too high, the glass substrate is melted and pattern formation becomes impossible. When the temperature is above or near the glass transition temperature of the resist polymer, typically about 200°C, the resist is evaporated or is caused to

outgas.¹ The evaporated polymer molecules contaminate the surface of the critical components of an electron beam writer to force it to repeat frequent parts replacement which eventually makes the writer unproductive. When the temperature is below a certain level, typically below 100°C, the resist heating effect results in CD error but it can be suppressed or corrected. The historical approach to suppress the resist heating effect has been constrained in two ways: either to increase the pass count to have a smaller exposure dose per one pass² or to re-route the writing path to travel a longer distance.^{3,4} But both remedies are not ideal as they both result in an increase in the writing time. It is desirable to correct CD error by the estimated temperature rise for each exposure unit.

In Sec. 2, we discuss how to model the temperature rise in VSB writing. We adopted a simple model to solve the heat diffusion equation in an analytic form. In Sec. 3, we discuss how to evaluate the resist heating effect by experiment and we show that the simple model explained in Sec. 2 is expressing the heating behavior with sufficient accuracy. In Sec. 4, we discuss how to correct CD error caused by resist heating and we propose that the correction by exposure dose is superior to the correction by size. We will also show the advantage of our correction scheme in the units of the tertiary (third) deflection field introduced from our EBM-9000 model.⁵ In Sec. 5, we discuss how much computational power is required to calculate the temperature rise and to correct the exposure dose but to still keep up with the writing speed. In Sec. 6, we demonstrate the correction accuracy by printed results with correction and show that our calculation runtime is shorter than the writing time by a fairly good margin.

*Address all correspondence to: Noriaki Nakayamada, E-mail: nakayamada.noriaki@nuflare.co.jp

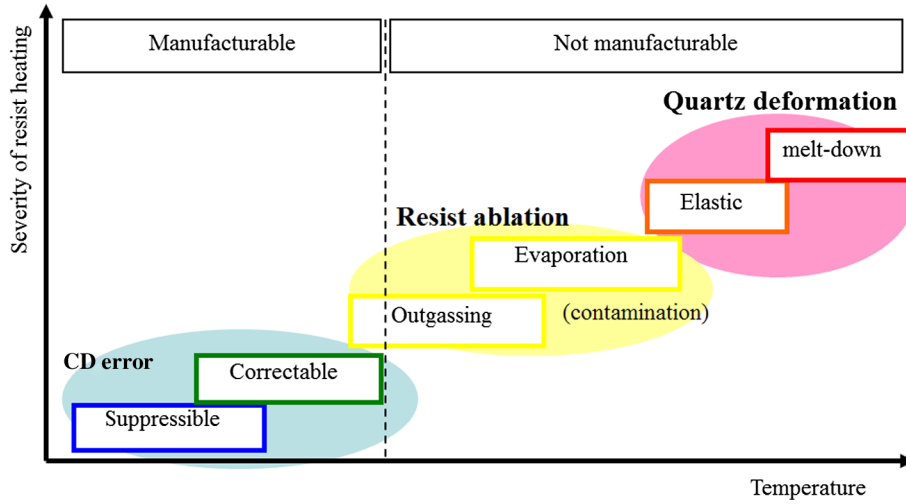


Fig. 1 Conceptual view of resist heating effect.

2 Modeling of Resist Heating

This section describes how we model the temperature rise for an individual exposure unit. General thermal diffusion is written in a form of parabolic partial differential equation:

$$\frac{\partial T}{\partial t} = k \left(\frac{\partial^2 T}{\partial x^2} + \frac{\partial^2 T}{\partial y^2} + \frac{\partial^2 T}{\partial z^2} \right) + Q, \quad (1)$$

where T is the temperature, t is the time, (x, y, z) are the spatial coordinates, and Q is the temperature rise ratio by electron exposure in unit time. k is called the thermal diffusivity and is denoted as

$$k = \frac{\lambda}{\rho C_p}, \quad (2)$$

where λ is the thermal conductivity, ρ is the mass density, and C_p is the specific heat capacity of the material in which the thermal diffusion occurs.

To simplify the thermal diffusion model, we follow Ralf's approach^{6,7} presented in Fig. 2.

- Only glass substrates exist, and any other layers such as resist or conductive materials beneath the resist and above the substrate are ignored.

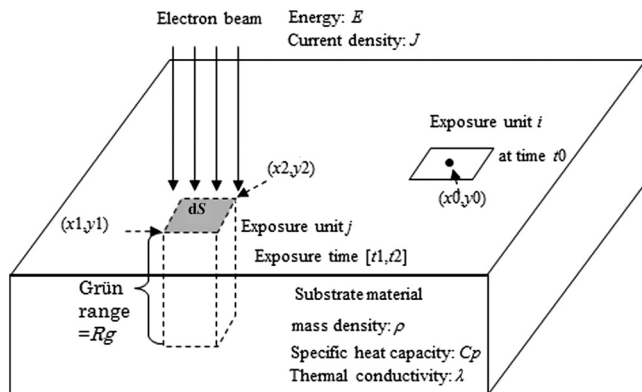


Fig. 2 Simplified thermal diffusion model.

- Heat is generated uniformly in the glass substrate in a bounded area by the incoming shot area in the (x, y) axes, from the top surface to the depth in the z -axis defined by the Grün range (R_g),

$$R_g = \frac{0.046}{\rho} E^{1.75}, \quad (3)$$

where E is the electron energy in the unit of kilovolts, ρ is defined in the unit of g/cm^3 , and R_g is given in the unit of micrometers.

With these simplifications, one can dictate the temperature transfer δT_{ij} from one rectangle exposure unit j to the other unit i as follows:

$$\begin{aligned} \delta T_{ij} = Q \int_{t_1}^{t_2} \text{erf} \left(\frac{R_g}{\sigma} \right) \cdot \frac{1}{2} \left\{ \text{erf} \left(\frac{x_0 - x_1}{\sigma} \right) - \text{erf} \left(\frac{x_0 - x_2}{\sigma} \right) \right\} \\ \cdot \frac{1}{2} \left\{ \text{erf} \left(\frac{y_0 - y_1}{\sigma} \right) - \text{erf} \left(\frac{y_0 - y_2}{\sigma} \right) \right\} dt, \\ Q = \frac{E \cdot J \cdot dS}{R_g \cdot \rho \cdot C_p \cdot dS} = \frac{E \cdot J}{R_g \cdot \rho \cdot C_p}, \\ \sigma = 2\sqrt{k(t_0 - t)}, \end{aligned} \quad (4)$$

where t_0 is the time to begin the exposure and (x_0, y_0) are the center coordinates of the exposure unit i , respectively. (x_1, y_1) is the origin, (x_2, y_2) is the upper right coordinates, and $[t_1, t_2]$ is the starting and ending times of the exposure unit j , respectively. Temperature rise T_i at the starting time and at the center coordinate of the exposure unit i is obtained by the sum of δT_{ij} for the total $(i - 1)$ exposure units written prior to the unit i as

$$T_i = \sum_{j=1}^{i-1} \delta T_{ij}. \quad (5)$$

Table 1 summarizes the physical properties of the glass substrate used in this paper.

Table 1 Summary of physical properties of glass substrate.

Property	Number	Unit
Mass density, ρ	2.22	g/cm^3
Specific heat capacity, C_p	0.772	$\text{J}/(\text{g} \cdot \text{K})$
Thermal conductivity, λ	1.38	$\text{W}/(\text{m} \cdot \text{K})$
Thermal diffusivity, k	0.805	$\mu\text{m}^2/\mu\text{s}$

3 Experimental Evaluation of Resist Heating

Figure 3 shows the basic design of the resist heating test chip. It is composed of a total 25 subfields in a 5×5 array. Each subfield has $9 \mu\text{m} \times 9 \mu\text{m}$ dimensions. Only the center subfield has metrology sites which are two cross patterns. Other 24 subfields are expected to give the heating load to the center sites. The nominal CD of the cross pattern is 200 nm and it is measured to evaluate the resist heating effect. The pattern density of the surrounding subfields is close to 100%.

In order to evaluate the resist heating effect, one must have a way to control the temperature rise to the warmer or to the cooler, ideally at any designed set point. As was described in Sec. 2, the gross effect of resist heating is proportional to the magnitude of Q which is the temperature rise in unit time. The absolute value Q itself is constant once the electron energy is set at 50 kV and the electron current density is fixed. However, the time average of incoming electrons, i.e., the average electron current, can be controlled by changing the beam parameters. In this paper, we use shot size and the shot settling time to control the average electron current. See Table 2 for the actual parameters used in the experiments. Additionally, we prepared several kinds of test chips to have multiple variations of writing orders so that we can evaluate how the resist heating is impacted by the writing order. We prepared two kinds of writing orders for the intersubfield perspective and three kinds of writing orders for the intrasubfield perspective, and they were paired with each other to make a total of six combinations. For the intersubfield perspective, we prepared “first-subfield” and “last-subfield” variations. See Fig. 4 for the details of writing orders together with the plot of temperature rise estimated by the model described in Sec. 2. In

Table 2 Summary of writing parameters.

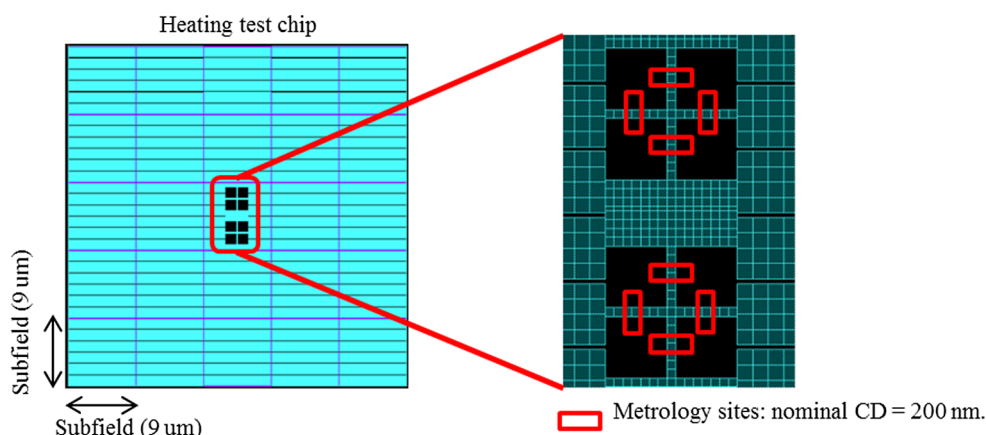
Writing tool	EBM-9500
Current density	1200 A/cm^2
Shot size variations	50, 100, and 200 nm
Settling time variations	12.8, 25.6, 48, and 200 ns
Resist	PRL009 (FUJIFILM)
Dose	22 $\mu\text{C}/\text{cm}^2$
Pass count	2

the first-subfield case, the subfields are written in spiral-out mode. In the last-subfield case, they are written in spiral-in mode. For the intrasubfield perspective, we prepared three variations which are “first-in-subfield,” “middle-in-subfield,” and “last-in-subfield” cases. See Fig. 5 for the details of writing orders with the plot of temperature rise.

The exposure was performed on NuFlare’s EBM-9500 operating at $1200 \text{ A}/\text{cm}^2$. Resist was PRL009 from FUJIFILM, exposed at $22 \mu\text{C}/\text{cm}^2$ with two passes. The cross patterns were measured by HOLON CD-SEM Z7.

Figure 6 shows the measured CD against estimated temperature rise. We were able to see the linear correlation between the CD and temperature. Correlation parameter was estimated as $0.05 \text{ nm}/\text{K}$. In Fig. 6(b), the data points are separately shown by first-subfield or last-subfield to indicate the intersubfield effect. In Fig. 6(c), data points are separately shown by the first-in-subfield, middle-in-subfield, or last-in-subfield to indicate intrasubfield effect. With the experimental conditions in Table 2, the intersubfield effect seems to be more dominant than the intrasubfield effect.

Although the good correlation between the measured CD and the estimated temperature is confirmed, this experiment itself does not exclude the possibility that the error comes from other sources which have time-dependent characteristics such as beam shaping drift. In this paper, we simply assume that the majority of the error comes from resist heating effect based on other technical evidence.⁸ Further

**Fig. 3** Chip design of resist heating test.

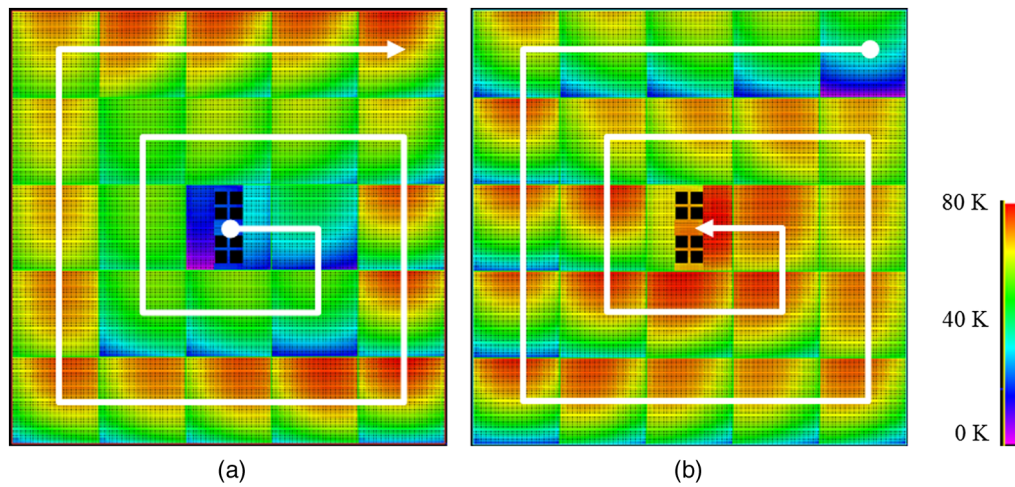


Fig. 4 Plot of temperature rise with writing order of subfields: (a) first-subfield and (b) last-subfield.

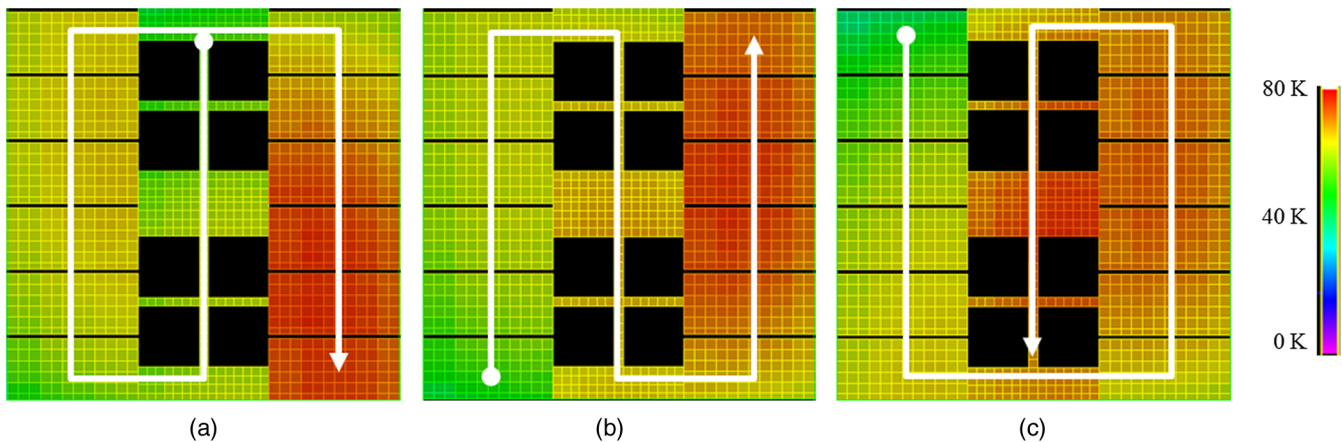


Fig. 5 Plot of temperature rise with writing order inside a subfield: (a) first-in-subfield, (b) middle-in-subfield, and (c) last-in-subfield.

segmentation tests should be planned to prove an such assumption is valid by excluding other error sources.

4 Discussions on How to Perform Resist Heating Correction

4.1 Dose Correction Versus Size Correction

Assuming that the correlation between the measured CD and estimated temperature is real and not coincidental, the next discussion is how to correct the CD error, whether by exposure dose or by feature size. After careful examination, we concluded that the correction by dose is superior to the correction by size. We explain the reason using a simple example. Suppose we have a $200 \text{ nm} \times 201 \text{ nm}$ pattern and it is divided into two $200 \text{ nm} \times 100.5 \text{ nm}$ shots with the maximum shot size limitation of 200 nm . Then we estimate a certain temperature rise to reduce its size, for example, by 1 nm . If we correct the feature size by -1 nm , the corrected pattern becomes $199 \text{ nm} \times 200 \text{ nm}$ which now can be written by one shot. Since the pattern division is reduced from two shots to one shot, it may increase the heating effect to require additional correction by -1 nm for example. Thus, the correction may be difficult to converge. On the other hand with the correction by dose, a -1 nm correction may need a -1% dose reduction for example. Certainly, there will be a

correction residual as the temperature rise will also be smaller by 1% from the original estimation. However, the residual of CD by this -1% temperature estimation error will result in only a -0.01 nm overcorrection. Therefore, we concluded that the correction by dose is superior to the correction by size. In case of dose correction, the correction residual should get recursively smaller, but the size correction has more impact on the change in the writing schedule and consequently on the change in the resist heating effect.

4.2 Correction Per-Shot Versus Per-Tertiary Field

As was explained by Eq. (5), the cost of temperature calculation for the total shot count of n is $1 + 2 + 3 + \dots + (n - 1) = n(n - 1)/2$. When n is a sufficiently large number, the cost is essentially proportional to the square of the shot count (n^2). The writing time is described in a simple equation such as

$$\text{Write time} = n[\text{Dose}/J + (\text{pass count}) \cdot (\text{settling time})] + \text{overhead}, \quad (6)$$

and it is proportional to the shot count in general. If we adopt a resist heating correction by the shot basis, it becomes

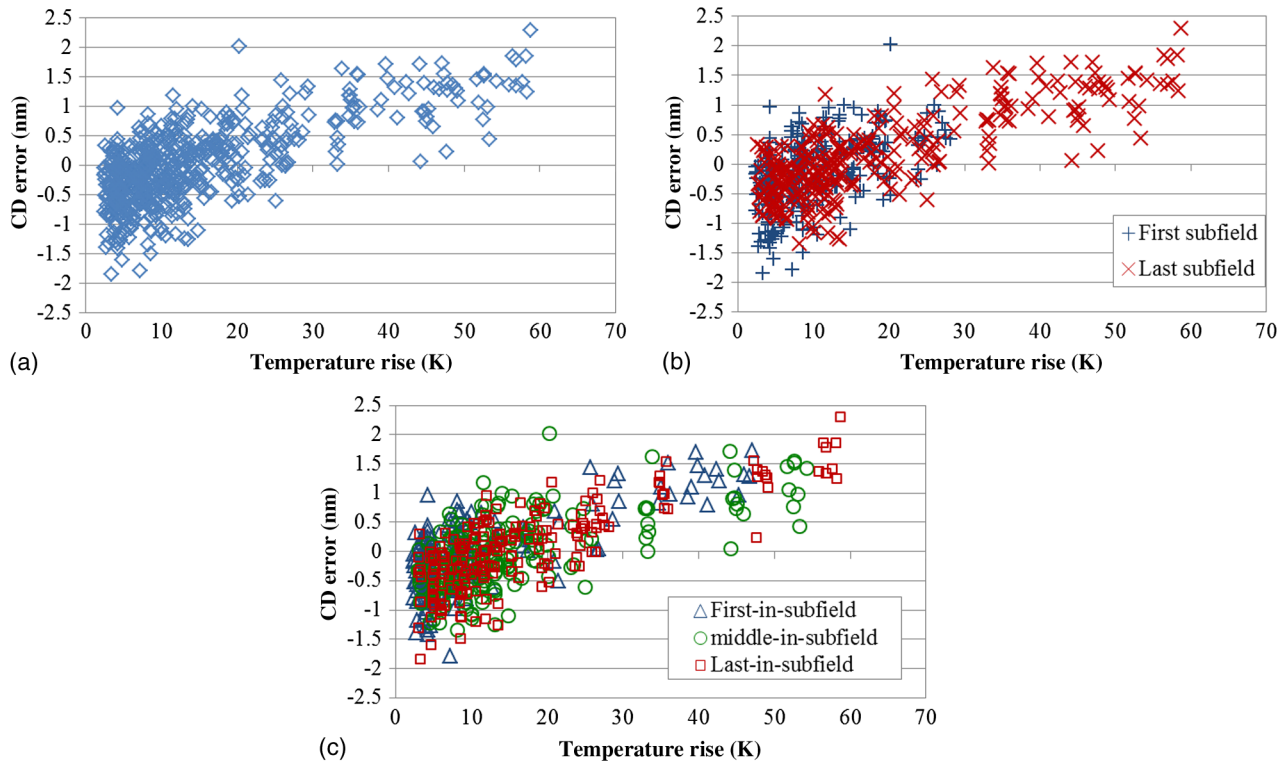


Fig. 6 Experimental results of resist heating effect: (a) overall plot, (b) separately plotted by intersubfield perspective, and (c) separately plotted by intrasubfield perspective.

significantly difficult for the calculation speed to catch up with the writing speed. Therefore, we decided to run the resist heating correction on a tertiary field basis (Fig. 7).

The advantages of running resist heating correction per-tertiary field are described as follows:

- Grouping of shots into a tertiary field should naturally reduce the total number of the elements to be corrected, which then reduces the calculation cost drastically.
- Once the tertiary field size is fixed, the number of tertiary fields is also capped as they cannot extend beyond the chip size. On the other hand, the shot count is not constrained by the chip size. With the per-tertiary field approach, it is easier to estimate the maximum calculation time than with the per-shot approach.

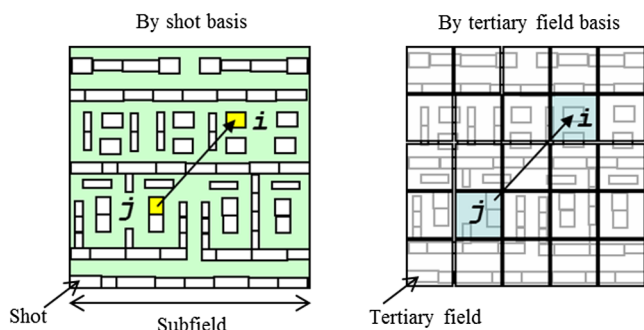


Fig. 7 Comparison of resist heating correction by shot basis versus tertiary field basis.

5 Computational Power Required for Resist Heating Correction

Even with the per-tertiary field correction, the fundamental ratio between writing time and calculation time stays the same as n to n^2 . Each EBM tool needs to be equipped with a huge computational power to finish resist heating correction before the writing needs the corrected shot data. Figure 8 shows the basic study in estimating how much computational power should be required for the resist heating calculation. We compared four metrics against the number of tertiary fields:

- Heating calculation time with one CPU with 10 cores (Intel Xeon E5-2690@3GHz).
- Heating calculation time with one graphical processing unit (GPU) chip (NVIDIA Kepler K10).
- Writing time of heavy layout with 2 T shots at $25 \mu\text{C}/\text{cm}^2$ per pass with $1200 \text{ A}/\text{cm}^2$ (average cycle time per-tertiary field is $2.2 \mu\text{s}$).
- Writing time of light layout with 500 G shots at $25 \mu\text{C}/\text{cm}^2$ per pass with $1200 \text{ A}/\text{cm}^2$ (average cycle time per-tertiary field is $0.6 \mu\text{s}$).

As can be seen in the graph, the light layout is more difficult to catch up with by the resist heating calculation as the number of shots in one tertiary field is smaller, so that the compaction of shots by the tertiary field works less effectively than it works on a heavy layout. If we target resist heating correction for $\sim 10^5$ tertiary fields, for example, it requires more than ~ 1000 CPU or ~ 100 GPU chips to catch up with the writing speed of a light layout. Adoption of GPU

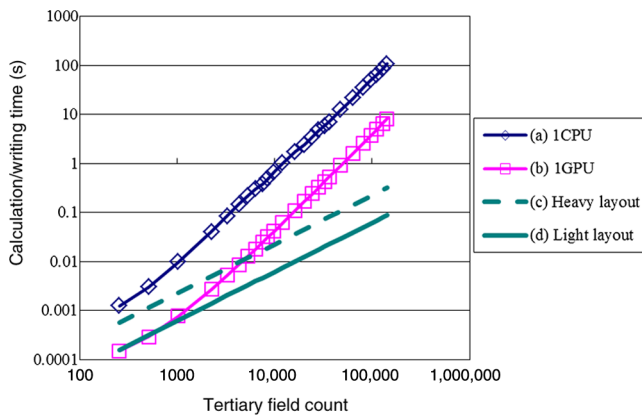


Fig. 8 Comparison of resist heating calculation time (a and b) versus writing time (c and d).

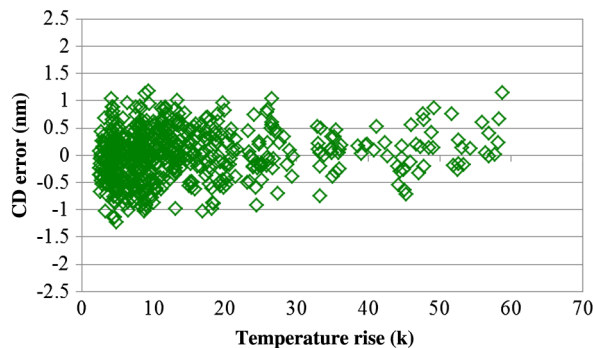


Fig. 9 Result of test chip print with resist heating correction.

technology is mandatory in the implementation of real-time correction. Our GPU cluster system called Computational Design Platform is equipped with more than 100 CPU and 200 GPU chips to suit that purpose perfectly.

6 Verification of Resist Heating Correction

6.1 Critical Dimension Accuracy

The test layout described in Sec. 3 was written with resist heating correction on the same EBM-9500 tool. The result is shown in Fig. 9 and summary of CD accuracy is shown in Table 3. The original CD 3sigma before correction (Fig. 4) was 2.0 nm. If the estimated temperature with best fitted scaling parameter, the estimated residual 3sigma was 1.4 nm. With the actual correction, the residual 3sigma was also 1.4 nm, meaning that the resist heating correction is working as designed.

6.2 Calculation Time

Figure 10 shows the datapath runtime on a typical light layout. The calculation time was normalized by the actual writing time. We compared the results between no correction (baseline) and with resist heating correction by 100, 160, and 196 GPU chips. In all conditions, the calculation time is shorter than the writing time by a good margin. With 100 GPU chips, it is slightly slower than the baseline without

Table 3 Summary of CD accuracy comparison between uncorrected and corrected results.

CD 3sigma	
Original result without correction	2.01 nm
Estimated residual	1.41 nm
Actual printed residual with correction	1.36 nm

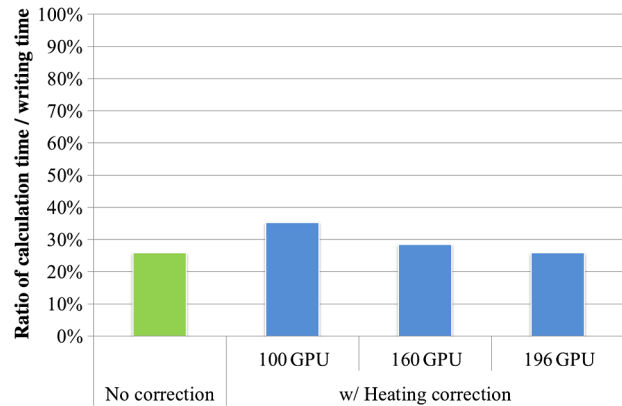


Fig. 10 Ratio of the datapath runtime to the writing time.

correction, but with 196 GPU chips, the difference can be suppressed to the negligible level.

7 Conclusion

We developed the resist heating correction system for our latest VSB mask writers EBM-9000/9500. We adopted a correction scheme per-tertiary field and GPU cluster system and achieved a correction runtime shorter than the writing time by a sufficiently large margin. With resist heating correction system, CD 3sigma can be reduced by about 30% while keeping the pass count as two so that the productivity does not have to be sacrificed. Resist heating correction system should remove the need for the tradeoff between CD accuracy and increased pass count, and it should promise the extended life of VSB mask writer until a multibeam mask writer is fully deployed in the production line.

Acknowledgments

The authors would like to thank Dr. Jun Yashima for his useful advice in experimental setup and for his skillful contribution in software implementation. They also thank Susumu Chiba for his continual support in CD-SEM measurements.

References

1. T. Abe et al., "Resist heating effect in direct electron beam writing," *J. Vac. Sci. Technol., B* 6(3), 853–857 (1988).
2. H. Sakurai et al., "Resist heating effect on 50 keV EB mask writing," *Proc. SPIE* 3748, 126 (1999).
3. K. Goto et al., "Reduction of resist heating effect by writing order optimization, part II," *Proc. SPIE* 6607, 660721 (2007).
4. S. Babin et al., "Resist heating dependence on subfield scheduling in 50 kV electron beam maskmaking," *Proc. SPIE* 5130, 718 (2003).

5. H. Takekoshi et al., "EBM-9000: EB mask writer for product mask fabrication of 16 nm half-pitch generation and beyond," *Proc. SPIE* **9256**, 925607 (2014).
6. H. I. Ralf, G. Duggan, and R. J. Elliot, *Proc. 10th Int. Conf. on Electron and Ion Beam Science and Technology*, p. 219, Electrochemical Society, Pennington, New Jersey (1982).
7. T. Kamikubo et al., "Study of heating effect on CAR in electron beam mask writing," *Proc. SPIE* **6607**, 660723 (2007).
8. S. Babin, "Measurement of resist response to heating," *J. Vac. Sci. Technol., B* **21**(1), 135–140 (2003).

Noriaki Nakayamada received his ME degree in nuclear engineering from the University of Tokyo, Japan. He joined Toshiba in 1993 and

moved to Toshiba Machine in 1996 to work on the development of the company's first commercial 50-kV VSB mask writer. For two decades, he has been working on the development of VSB mask writers to the latest model. His major achievement was the introduction of correction software for the resist surface charging effect.

Mizuna Suganuma received her BS and MS degrees at Tokyo University of Science in 2010 and 2012, respectively. She joined NuFlare Technology Inc. in 2012 and has been working on the development of resist heating correction.

Biographies for the other authors are not available.